

Wire-Free Tactile Sensing Element Based on Optical Connection

*Kouichi Yamada, **Kenji Goto, *Yoshiki Nakajima, *Nobuyoshi Koshida,
and **Hiroyuki Shinoda

*Tokyo University of Agriculture &
Technology 2-24-16 Koganei, Tokyo
184-8588 Japan
ykou@cc.tuat.ac.jp

**The University of Tokyo, 7-3-1
Hongo, Bunkyo-ku, Tokyo 133-0033
Japan
shino@alab.t.u-tokyo.ac.jp

Abstract

An idea of wireless tactile sensing chip using RF connection has been proposed for realizing a soft artificial robot skin. However, it is difficult to make the RF tactile sensing element smaller than several millimeters because the energy transmission efficiency decreases as the coil size becomes smaller. In this paper we propose a wireless tactile sensing element based on optical connection. The sensing chip with 1 mm cubic shape operates with optical power, and sends optical codes of 6 stress components measured by an optical sensing method. We describe the chip design and the 6 stress sensing principle, and show experimental results of the stress sensing using a prototype of a 4 mm cubic chip. Then we estimated the required optical power for the sensing chip, and checked the operation of the digital circuit on the chip.

Key Words: Tactile Sensor, Artificial Skin, Sensitive Skin, Wireless measurement, Optical Connection

1 Introduction

A key idea for realizing an elastic tactile sensing device that can sense as a human does, is removing metal wires. A former paper presented a wireless tactile sensing chip using inductive connection for receiving and transmitting power and signal [1]. However, it is difficult to make a tactile sensing element smaller than several millimeters because the energy transmission efficiency decreases as the coil size becomes smaller.

In this paper we propose a wireless tactile sensing element based on optical signal transmission. The sensing chip in 1mm cubic shape operates with optical power, and sends optical codes of 6 stress components measured by an optical sensing method. We describe the chip design and the principle of stress detection, and show experimental results using a 4 mm prototype sensor chip. We estimated the required optical power, and examined the chip operation.

2 Tactile Sensing Based on Optical Connection

A schematic diagram of an artificial skin we propose here is shown in Fig. 1. Each tactile sensing chip is embedded with 2 millimeter interval in a soft artificial

robot finger. The transparent robot skin allows optical connection between the sensor chip and the optical transmitter/receiver located inside the finger. Each sensor chip operates with the optical power from the transmitter (LED). Meanwhile this light also becomes optical signals from a computer. In addition, the stress on a sensor chip is measured from the intensity change of the LED light detected inside the sensor chip. The sensor chip emits light digital signals with porous silicon formed on it [2] that is detected by the external optical detector.

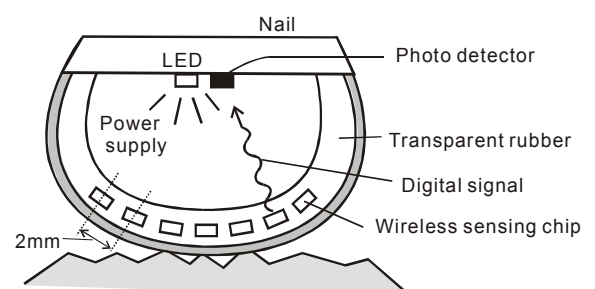


Fig. 1: Schematic diagram of a sensor skin using optical tactile sensing elements.

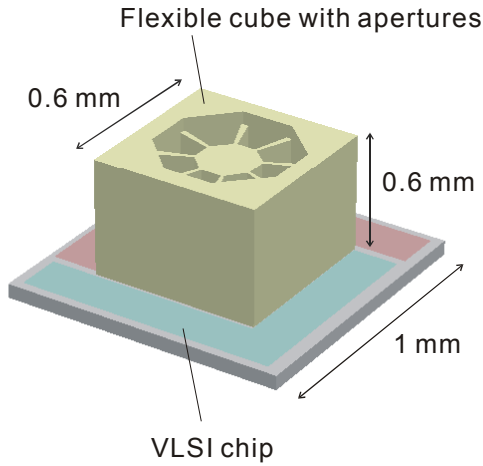


Fig. 2: Structure of the optical tactile sensing element.

3 Wire-Free Optical Tactile Sensing Element

The structure of the sensing chip is shown in Fig. 2. The sensor chip consists of two parts. One is a VLSI chip for receiving optical power with PN Junction, measuring optical intensity on it, and signal processing. The other is a flexible cube with apertures attached onto the VLSI chip for measuring 6 components of stress around the chip.

The layout of the VLSI chip is shown in Fig.3. The surface is shared with a solar cell of PN junction for receiving optical power, a porous silicon luminescer formed on the VLSI chip, a signal processing part, and photo diodes.

This VLSI chip was made in ROHM 0.35mm process that is supported by VDEC (VLSI Design and Education Center) at the University of Tokyo.

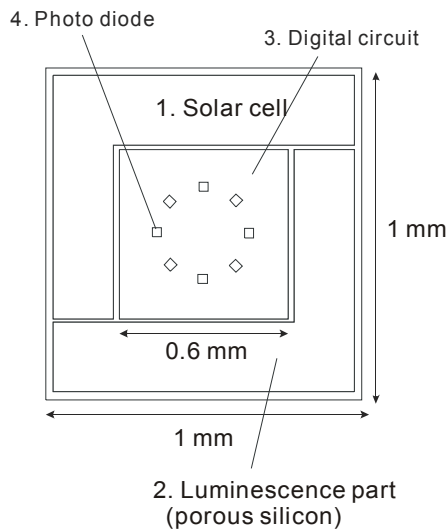


Fig. 3: Layout of the VLSI chip

4. Method of Stress Measurement

Since what is the essential stress component in tactile sensing is still unclear, it is desirable our device can sense all components of stress tensor. Because the sensor chip with VLSI circuit can measure light intensity at multiple points, it is possible to detect 6 components of stress tensor theoretically.

Structure of a flexible cube attached to the LSI chip is shown in Fig. 4. It is a 0.6 mm cube that has 8 holes to the photo diodes. The holes 1, 3, 5, and 7 have the same structure that has symmetrical projections on the facing walls inside the hole as is shown in Fig. 4. Meanwhile the holes 2, 4, 6, and 8 have projections attached at different heights on the walls. The sensor detects the deformation of the flexible cube from the intensity change at the photodiodes. The photodiodes 1, 3, 5, and 7 detect shearing/normal stress σ_{xz} , σ_{yz} , σ_{xx} and σ_{yy} applied to the cube using the symmetry. Here σ_{xx} expresses normal stress along the x axis, and σ_{xz} expresses shearing stress that is tangential force along x axis on the top surface of the cube.

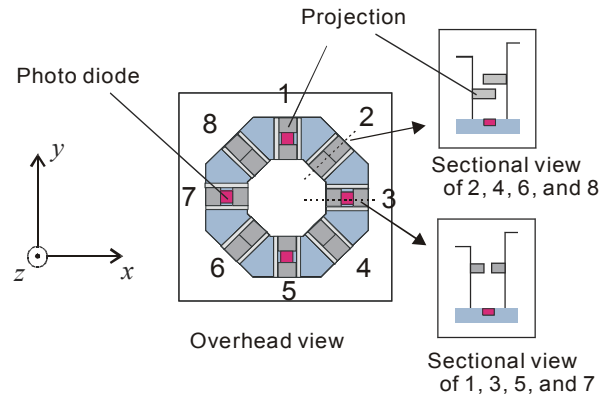


Fig. 4: Structure of the flexible cube with apertures.

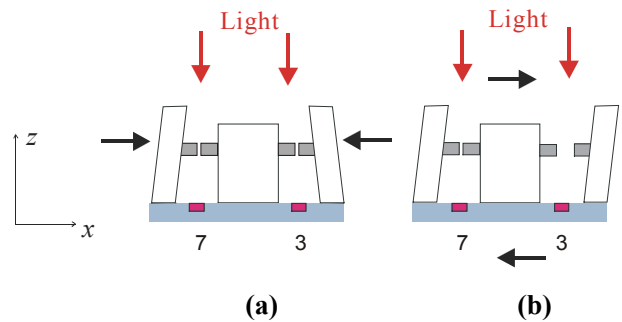


Fig. 5: Sensing normal stress σ_{xx} and shearing stress σ_{xz} .

The principle is explained in **Fig. 5**. The holes 3 and 7 deform symmetrically for the normal stress along the x axis, while they deform antisymmetrically for the shearing stress σ_{xz} .

Therefore we can obtain equations using constants A , B , C , and D as follows.

$$dp_3 + dp_7 = A\sigma_{xx} + B\sigma_{yy} + C\sigma_{zz} \quad (1)$$

$$dp_3 - dp_7 = D\sigma_{xz} \quad (2)$$

The dp_i ($i=3,7$) is the light intensity change detected at the photo diode i . The absolute values of the coefficients $|B|$ and $|C|$ are smaller than $|A|$. From the symmetry we can also obtain

$$dp_1 + dp_5 = A\sigma_{yy} + B\sigma_{xx} + C\sigma_{zz} \quad (3)$$

$$dp_1 - dp_5 = D\sigma_{yz} \quad (4)$$

using the same parameters A to D .

The 5th stress σ_{xy} is illustrated in Fig.6. Shearing stress is applied to the side walls. In this case, the light intensity at point 4 and 8 increases, and that at point 2 and 6 decreases. From this symmetry, we can write as

$$dp_4 + dp_8 - (dp_2 + dp_6) = E\sigma_{xy} \quad (5)$$

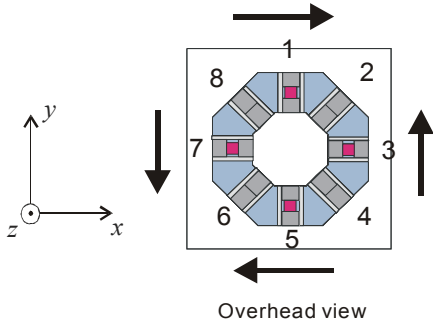


Fig. 6: Sensing shearing stresses σ_{xy} .

The last 6th stress σ_{zz} , the vertical normal stress is illustrated in Fig. 7. The gap distance between the facing projections are mainly sensitive to the normal stress σ_{zz} . Then the parameter G in

$$dp_2 + dp_4 + dp_6 + dp_8 = F\sigma_{zz} + G(\sigma_{xx} + \sigma_{yy}) \quad (6)$$

is smaller than F .

The equations (1), (3), and (6) give the normal stress σ_{xx} , σ_{yy} , and σ_{zz} . If we neglect B , C , and G , we can simply write

$$\begin{pmatrix} \sigma_{xx} \\ \sigma_{yy} \\ \sigma_{zz} \end{pmatrix} = \begin{pmatrix} (dp_3 + dp_7) / A \\ (dp_1 + dp_5) / A \\ (dp_2 + dp_4 + dp_6 + dp_8) / F \end{pmatrix} \quad (7)$$

$$\begin{pmatrix} \sigma_{xz} \\ \sigma_{yz} \\ \sigma_{xy} \end{pmatrix} = \begin{pmatrix} (dp_3 - dp_7) / D \\ (dp_1 - dp_5) / D \\ (dp_4 + dp_8 - dp_2 - dp_6) / E \end{pmatrix}. \quad (8)$$

From above equations, we obtain the all components of stress tensor σ_{ij} .

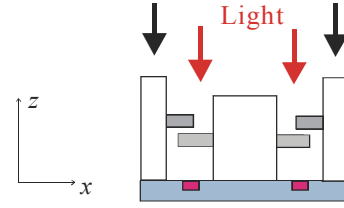


Fig. 7: Sensing vertical normal stress σ_{zz} .

5. Experiments of Stress Sensing

We fabricated prototypes of flexible cube using elastic silicone rubber (Young's modulus $\approx 10^5$). The edge length of the cube is 4 mm. This prototype has only 4 slits with 0.2 mm gap for detectors 1, 3, 5, and 7.

We located the flexible cube so that No. 3 and 7 in Fig. 8 are along the x axis. And we observed the light intensity at detector 3 when we applied σ_{xx} and σ_{zz} . The plots 'x-stress' in Fig. 9 shows normalized output p/p_0 when we applied horizontal compressive force to the cube faces perpendicular to the x axis with no stress to other faces. The 'strain' of the horizontal axis means the ratio of the deformed cube length along the x axis to the original length. The plots 'z-stress' show the detector's output when we applied vertical compressive force to the horizontal cube faces with other faces free. For these plots the strain means the ratio of the deformed cube length along the z axis to the original length. Plots show the detector 3 is more sensitive to horizontal normal stress than to vertical one that implies A in Eq. (1) is larger than B .

The plots in Fig. 10 show the normalized output of 3 and 7 when we applied shearing deformation. The 'strain' of the horizontal axis means the shearing strain

$$u_{xz} = \frac{1}{2} \left(\frac{du_z}{dx} + \frac{du_x}{dz} \right) \quad (9)$$

where $\mathbf{u}(\mathbf{r}) = (u_x, u_y, u_z)$ is the displacement vector at \mathbf{r} of the cube body. The figure shows the slopes of 3 and 7 have opposite signs to each other. These results show the 4 slit

detectors can resolve applied stress into σ_{xx} , σ_{yy} , σ_{xz} , and σ_{yz} if we neglect the effect from σ_{zz} . If we add one output that is sensitive to σ_{zz} , exact resolution of the stress into the components becomes possible.

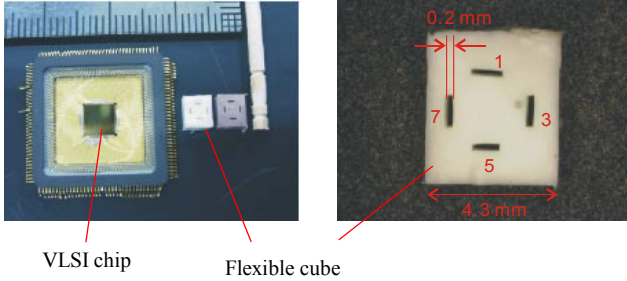


Fig. 8: (a): A photograph of a VLSI chip for our prototype sensor chip. (b): A photograph of a flexible cube for 4-component stress measurement.

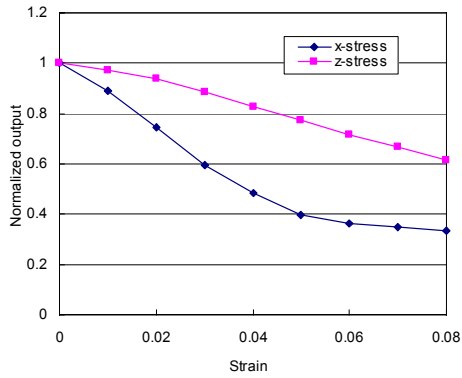


Fig. 9: Normalized output of photodiode 3 when horizontal compressive force and vertical compressive force are applied to the prototype sensor chip. The ‘strain’ for ‘x-stress’ and ‘z-stress’ implies the ratio of the deformed cube length along the x and z axis, respectively, to the original length.

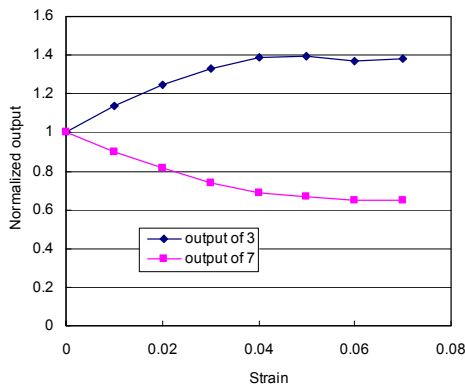


Fig. 10: Normalized output of photodiode 3 and 7 when shearing strain is applied to the prototype sensor chip.

6. LSI Chip Operation and Power Consumption

In our design, the VLSI chip operates at 10 MHz and transmits 8×6 bit stress data with 1 MHz signal frequency. Signal transmission time for one chip is within 100 μ sec. All the chips obtain unique IDs at the beginning of the operation using random number generator, and respond to the commands with ID transmitted from the LED.

Each chip obtains one sample of stress data by measuring the photon charge generating for 1 ms. Though we have not confirmed the energy consumption of the chip experimentally, we suppose the main power will be consumed by the logic circuit for communication. If we assume 0.1 μ W/MHz/gate, the average power consumption of our 10 thousand-gate logic circuit (0.5 mm square under the 0.35 μ m rule) is estimated at 100 μ W. If solar cell efficiency is 10 %, a 0.6 mm² solar cell needs 1.5 mW/mm² light intensity, which Laser can provide.

We are now examining the VLSI chip operation. The lower waveform in Fig. 11 is the response signal of our VLSI chip to test input. In our plan, the output signal form the circuit will be connected to a porous silicon luminescer formed on poly-silicon layer on the chip [2].

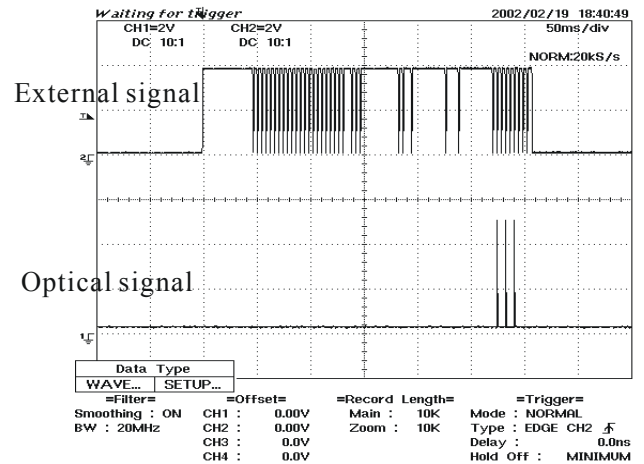


Fig. 11: An output signal from a VLSI chip for a test input signal.

References

- [1] H. Shinoda and H. Oasa: Wireless Tactile Sensing Element Using Stress-Sensitive Resonator, IEEE/ASME Trans. on Mechatronics, Vol. 5, No. 3, pp. 258-265, 2000.
- [2] Y. Nakajima, A. Kojima, and N. Koshida: A solid-state light-emitting device based on excitation of ballistic electrons generated in nanocrystalline porous poly-silicon films, Jpn. J. Appl. Phys., Vol. 41, 2002 (in press).